

Reinforcing optimization enabled interactive approach for liver tumor extraction in computed tomography images

Jayanthi Muthuswamy¹, Chanda Verabadra Reddy², Rekha Narayanaswamy²

¹Department of Electronics and Communication Engineering, New Horizon College of Engineering, Bengaluru, India

²Department of Electronics and Communication Engineering, Kammavari Sangham Institute of Technology, Bengaluru, India

Article Info

Article history:

Received Sep 8, 2022

Revised Jan 9, 2023

Accepted Jan 14, 2023

Keywords:

Computed tomography

Fuzzy C means

Median filter

Optimization

Segmentation

ABSTRACT

Detecting liver abnormalities is a difficult task in radiation planning and treatment. The modern development integrates medical imaging into computer techniques. This advancement has monumental effect on how medical images are interpreted and analyzed. In many circumstances, manual segmentation of liver from computerized tomography (CT) imaging is imperative, and cannot provide satisfactory results. However, there are some difficulties in segmenting the liver due to its uneven shape, fuzzy boundary and complicated structure. This leads to necessity of enabling optimization in interactive segmentation approach. The main objective of reinforcing optimization is to search the optimal threshold and reduce the chance of falling into local optimum with survival of the fittest (SOF) technique. The proposed methodology makes use of pre-processing stage and reinforcing meta heuristics optimization based fuzzy c-means (FCM) for obtaining detailed information about the image. This information gives the optimal threshold value that is used for segmenting the region of interest with minimum user input. Suspicious areas are recognized from the segmented output. Both public and simulated dataset have been taken for experimental purposes. To validate the effectiveness of the proposed strategy, performance criteria such as dice coefficient, mode and user interaction level are taken and compared with state-of-the-art algorithms.

This is an open access article under the [CC BY-SA](https://creativecommons.org/licenses/by-sa/4.0/) license.



Corresponding Author:

Jayanthi Muthuswamy

Department of Electronics and Communication Engineering, New Horizon College of Engineering

Bangalore, India

Email: jayanthisathish1012@gmail.com

1. INTRODUCTION

The liver [1] is the second-largest internal organ in human body. It helps to keep the human body free of toxins and toxic substances, helps to maintain body's metabolic balance. It is found in the abdomen upper right quadrant and weighs one and a half kilograms. The liver has many activities, including blood filtration, synthesis of protein, processing nutrients and fats, storing carbohydrates and transforming harmful substances into water solvable compounds. It is additionally inclined to a few kinds of liver ailments. The World Health Organization (WHO) [2] conducted statistical research on liver illnesses and concluded that it is one of India's most common ailments. Liver diseases can be identified with different colors for example brown for fibrosis yellow for fatty liver and blue for cyst.

Medical imaging [3] is a well-known technology used to view and examine the internal parts of the human body. This imaging provides a detailed informative mapping of a subject's anatomy. Because this imaging is primarily utilized for diagnosis, it is also known as diagnostic imaging. To diagnosis a specific problem in the human body, medical experts have used therapeutic hardware tools for image analysis. But

advanced imaging hardware and information processing have led to many techniques to find liver disorder. Additionally, imaging helps the Doctors to visualize and analyze the abnormalities in internal structures of liver.

The manual segmentation [4] of the liver takes a long time to find abnormalities and less accurate. Not only that segmentation results vary from experts to experts. Sometimes, human interpretation leads to false positive error and increase the possibility of false identification of tumor. Hence segmentation of liver is a fundamental step for the identification of liver syndrome, interpretation of complex interior structure and volume measurement of liver. Thus, segmentation proves to be very valuable in this situation. So, there is a demand of computer assisted system to extract the liver contour and to visualize the suspicious abnormal area inside the contour region.

Researchers are still struggling with how to precisely partition the liver and tumor regions. Over the years, researchers have produced enormous methodologies and approach to dissociate the liver and tumor from abdominal computerized tomography (CT) scans. Diaz *et al.* [5] presented systematic summary to pick from the variety of tools and platforms that are currently accessible to prepare medical images for developing or deploying artificial intelligence (AI) algorithms. The accurate, automated, simultaneous segmentation of the liver and hepatic tumors from CT images, [6] is suggested using a pipelined approach. The newly introduced structure has three tiers that are pipelined together and provide dice similarity coefficients 93.5%. Elmenabawy *et al.* [7] made attempt to explore the enhancements in classification accuracy. They have used a hybrid combination of spatial domain and prior to feature extraction, wavelet filtering is applied to the images in order to improve the accuracy.

Soft computing-based meta-heuristic optimization methods have also been the subject of extensive research. An autonomous liver segmentation system was proposed by Wu *et al.* [8]. Their technique used single-block linear detection algorithm (SBLDA) and produced liver segmentation with good execution time for low contrast CT images. Ali *et al.* [9] presented a new strategy to address the challenge of liver segmentation based on CT images using nature-inspired optimization. They have shown how segmentation can be resolved by using nature-inspired algorithms. A computer aided detection (CAD) for CT images of abdomen was presented in [10]. Sayed *et al.* [10] have developed a hybrid approach to lower the false positive error rate. Mirjalili *et al.* [11] elongated an improvised grey wolf optimization strategy for biomedical issues and the performance was contrasted with that of existing meta-heuristic optimization algorithms. Kumar *et al.* [12] proposed different techniques to identify the region of interest. In [13], a pipelined structure was developed for simultaneous segmentation of the liver and hepatics cancer images. In their work, Vo *et al.* [13] has used multiple filters to extract multiple features. In [14], a new swarm intelligence information approach for skin lesions segmentation have discussed for generating optimum segmentation that can be applied to a variety of images with varying possessions and deficiencies using a multistep pre-processing stage. A unique automatic liver segmentation approach was created in [15]. A smart operator was used for creating both the morphology and the volume of the liver and this method was performed well, allowing for exact 3D liver segmentation.

As can be seen, there are various approaches for extracting the liver contour. For separation of liver outline from CT scans of abdomen, a few of the techniques are addressed in the literature survey have used prior information of the area concerned and a solitary segmentation method. Fake segmentation errors can occasionally be produced by these means. The limitations of previous methods are discussed in the following section, with how the suggested technique is used for liver and tumor separation in computer-assisted systems. The following are some implications of liver segmentation issues: i) automatic liver segmentation is challenging since the liver overlaps with nearby organs and its intensity is similar to that of other organs; ii) to find the liver contour, existing approaches used pixel-based distribution; and iii) the majority of researchers concentrated on a single segmentation technique; however, this technique was unable to address complicated issues such patient-specific variations in liver shape.

The suggested study integrates machine learning with enhanced techniques to boost the effectiveness of segmentation results. So, the main objective of the proposed work is “to develop optimized system to delineate liver boundaries and to view the formation of tumor region in the liver in order to increase the segmentation accuracy and predict the tumor/lesion growth in liver”.

The suggested solution is an improvement of our previous hybrid approach to the problem of liver diagnostics [16]. We emphasized the significance of hybrid methods for extracting liver shape. As a result, in this proposed solution, we stress the importance of bio-inspired optimization techniques to choose the best threshold that radiologists can use in order to retrieve the liver shape. The steps of the suggested framework are as follows: Figure 1 depicts the entire framework that includes data acquisition, preprocessing, combined segmentation and optimization algorithm and post processing. Fuzzy c-means (FCM) is one of the most often used segmentation algorithms, in which each item can belong to multiple groups (thus the term "fuzzy"). However, this technique is susceptible to falling into local minima when selecting the cluster center. The FCM method is used with the grey wolf optimization technique to solve this flaw. This method is used to identify the best threshold by optimizing the cluster center. This method provides interactive hybrid method to select

the optimal threshold for the visualization of tumor contour in abdominal liver CT images. In hybrid segmentation phase, we have focused on two approaches in order to study which hybrid method provides the fine segmentation results.

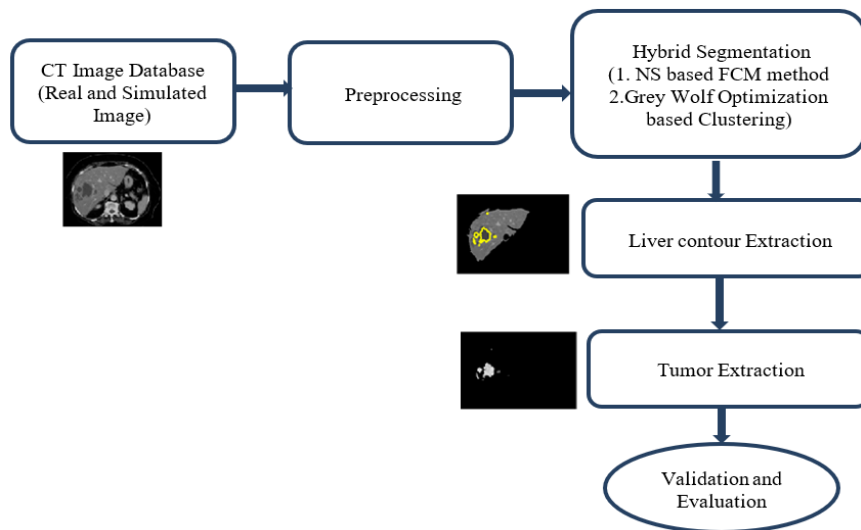


Figure 1. Computer assisted tumor extraction framework

2. METHOD

2.1. CT image database

Two types of CT image database are used in this work. One is real-time database and another is simulated database [17]. These images can be acquired in three different planes: sagittal, coronal, axial planes. These planes are used to describe the position of body parts. This also helps to find the extent of disease in a patient. Figure 2 shows image reconstruction plane of a patient and abdominal CT image view of all three planes [18]. Figure 2(a) depicts the sagittal view and Figure 2(b) illustrates how coronal plane divides the human body into front and rear. Figure 2(c) explains how the Superior and Inferior part of human body can be viewed through Axial plane.

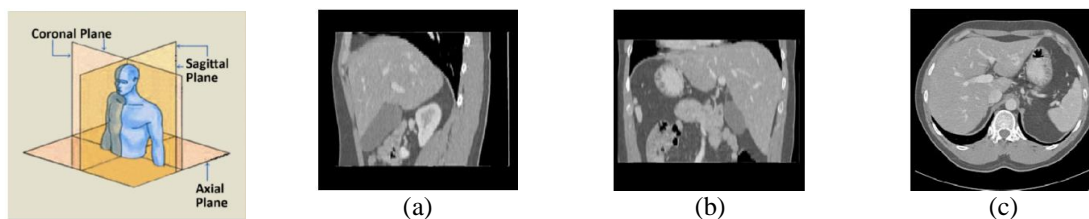


Figure 2. Image reconstruction (a) CT image view of 3 planes [18]-sagittal (b) coronal, and (c) axial

2.2. Preprocessing

Images of the abdominal region are captured by the CT scanner's that uses various sensors. These images are completely corrupted and affected by various noises [19], [20]. Gaussian and poisson noise are the two main sources of noise in CT imaging. Due to the combined effects of patient movement, insufficient sensor temperature, and poor light level intensity during the acquisition process, Gaussian noise occurs more frequently in CT images. The effectiveness of segmentation, feature extraction, and classification is impacted by noisy images. Low-quality images are ineffective for computer assisted systems, which produces unreliable results. Therefore, removing noise from abdominal CT scans is necessary for making the right diagnosis. In this work, we have used a simple preprocessing algorithm to remove the noise. For this median filter is taken. A median filter [21] is a nonlinear filter used for noise reduction. These filters are efficient in removal of noise, blurring effect and preserve the edges of an image.

2.3. Fuzzy c-means algorithm

The most well-known iterative clustering technique is FCM [22], [23]. The fuzzy c-means clustering algorithm calculates the cluster centers and the membership matrix (UM), and then minimizes an objective function J with regard to these cluster centers and membership degrees. Partitioning a set of data $DX=DX_1, DX_2, \dots, DX_M$ into 'C' number of clusters is the core idea. Based on the distance between the cluster and the data point, this algorithm determines each data point's membership in relation to each cluster center. The Pseudo code for FCM is given in Table 1.

Table 1. Pseudo code for FCM

Requirement: Decide the number of cluster C, the degree of fuzziness $m > 1$ and error ϵ	
1. Initialize the center of the cluster $CV_i^{(0)}$ and $UM_{ij}^{(0)}$ matrix.	
2. Set $k=1$	
3. At K step; Calculate the centers vectors $CV^{(k)}$ with $UM^{(k)}$	
(1)	
$CV_j = \frac{\sum_{i=1}^N UM_{ij}^m \cdot DX_i}{\sum_{i=1}^N UM_{ij}^m}$	
4. Update $UM^{(k)}$ and $UM^{(k+1)}$	
(2)	
$UM_{ij} = \frac{1}{\sum_{k=1}^C \left(\frac{\ x_i - CV_j\ }{\ x_i - CV_k\ } \right)^{\frac{2}{m-1}}}$	
5. If $UM^{(K+1)} - UM^{(k)} < \epsilon$ then stop. Otherwise return to step 3.	

2.4. Neutrosophic sets (NS) based FCM method

2.4.1. NS image

The image pixel $Im_Pi(m, n)$ is transformed into the Neutrosophic domain [24], [25] $NSI_Do(u, v) = \{Tru(u, v), Inm(u, v), Fal(u, v)\}$ where $Tru(u, v), Inm(u, v), Fal(u, v)$ are the probabilities belonging to the white set (object), indeterminate set (edge), and non-white set (background), respectively. The block diagram of NS based FCM method is shown in Figure 3. NS image is described mathematically by the (3) to (6).

$$Tru(u, v) = \frac{\overline{g(u, v)} - g_{min}}{g_{max} - g_{min}} \tag{3}$$

$$Inm(u, v) = 1 - \frac{(\overline{Hom(u, v)} - \overline{Hom_{min}})}{(\overline{Hom_{max}} - \overline{Hom_{min}})} \tag{4}$$

$$Hom(u, v) = abs(g(u, v) - \overline{g(u, v)}) \tag{5}$$

$$Fal(u, v) = 1 - Tru(u, v) \tag{6}$$

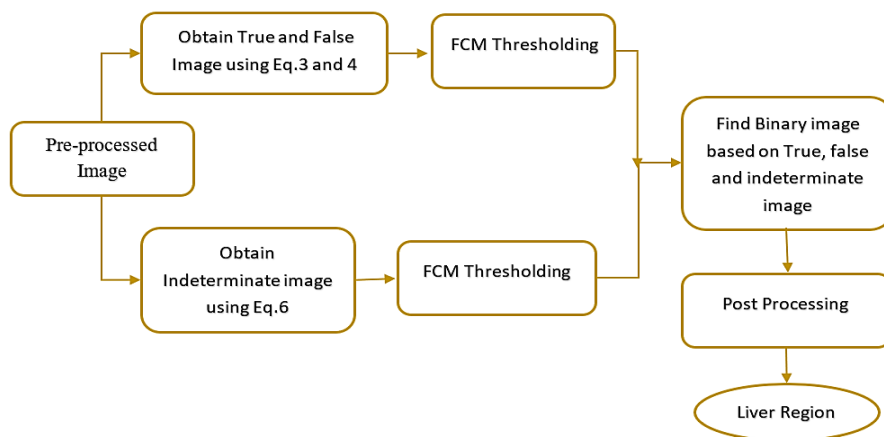


Figure 3. Block diagram of NS based FCM method

2.5. Optimization based meta heuristics - grey wolf optimization (GWO) algorithm

Optimization based Meta heuristics algorithm [26]–[28] is used to determine the optimal solution of the problem under consideration. Single solution-based and population-based algorithms are the two categories under which this method falls. The first method starts with one solution and improves the accuracy of the solution by means of the iteration process. The second category uses a set of solutions and improves the solutions through a fixed number of iterations. In the proposed work, population-based algorithm is used.

Bio-inspired GWO algorithm is used as a clustering technique to segment liver contour in CT images. Grey wolf algorithm has the advantage of being simple implementation, easy to program, and not requiring specific inputs. Grey wolves exist in packs, each with an average of 5-10 members. The leadership hierarchy is simulated using four varieties of grey wolves: alpha (α), beta (β), delta (δ), and omega (ω). The alpha wolves are the leaders, and their job to make decisions. Beta wolves are second-level wolves who assist alpha wolves in making decisions or performing other tasks. Delta wolves carry out orders of alpha and beta wolves and can also direct other underneath individuals. The omega wolves are in charge of leading the hunt (hunting) while the other wolves follow. Encircling, hunting, and attacking are the three steps of hunting behavior.

Grey wolves' mathematical formulation is utilized to construct social hierarchy behavior. The alpha represents the best fittest solution. The second and third fittest solution is beta and delta. There are multiple steps in grey wolf optimization before the prey is caught. In order to search the prey, random initialization of grey wolves in the search space is made. Following the detection of prey, the encirclement of prey begins. The mathematical aspects of encirclement are as (7) and (8).

$$D = C * X_{prey_pos}(t) - X_{grey_wp}(t) \tag{7}$$

$$X(t + 1) = X_{prey_pos}(t) - A.D \tag{8}$$

where 't' denotes the current iteration, $X_{prey_pos}(t)$ is the prey's position vector and $X_{grey_wp}(t)$ is grey wolf vector position. The coefficient vectors A and C are provided by (10).

$$A = 2ar1 - a ; C = 2r2 \tag{10}$$

where $r1$ and $r2$ are random vectors selected from the range [0, 1] and over the period of iteration, the value of 'a' decreases linearly from 2. The implementation flowchart is shown in Figure 4.

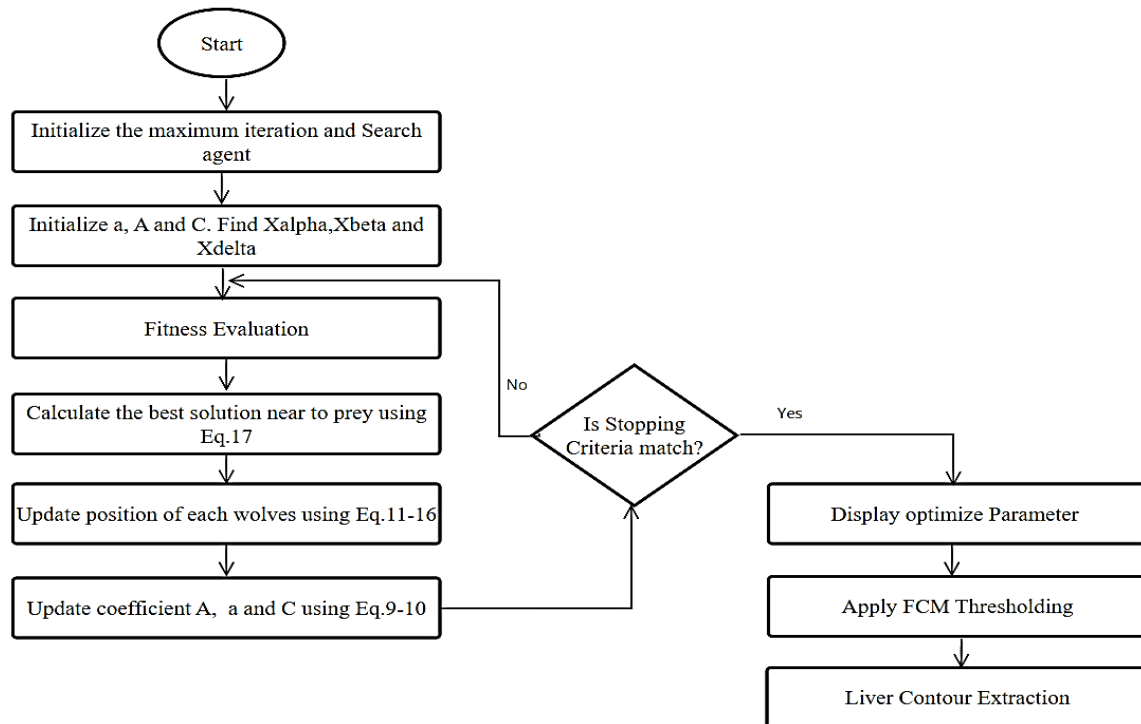


Figure 4. Implementation procedure of GWO based clustering

In hunting process, the best solutions from alpha, beta and delta are saved and the omega wolf update their positions in accordance with the best hunting solutions.

$$D_{alpha} = |C_1 \cdot X_{alpha}(t) - X_{grey_vp}(t)| \quad (11)$$

$$D_{beta} = |C_2 \cdot X_{beta}(t) - X_{grey_vp}(t)| \quad (12)$$

$$D_{delta} = |C_3 \cdot X_{delta}(t) - X_{grey_vp}(t)| \quad (13)$$

$$X_{1p} = X_{alpha}(t) - A_1 D_{alpha} \quad (14)$$

$$X_{2p} = X_{beta}(t) - A_2 D_{beta} \quad (15)$$

$$X_{3p} = X_{delta}(t) - A_3 D_{delta} \quad (16)$$

$$X(t+1) = \frac{X_{1p} + X_{2p} + X_{3p}}{3} \quad (17)$$

where $X_{grey_vp}(t)$ indicates the grey wolf vector position while D_{alpha} , D_{beta} , D_{delta} are distance between α , β and δ wolves with other individuals. $X_{alpha}(t)$, $X_{beta}(t)$, $X_{delta}(t)$ are the positions of alpha, beta and delta wolves at the iteration of 't'.

2.6. Liver contour and tumor extraction

The output of optimization method is a binary image. Later, post processing [29] is applied on this image to get the final segmented liver contour. The largest connected components are found, and the remaining gaps are filled using morphological processing. By overlaying the original image on the contour, we can determine the region of interest. By multiplying the liver mask with the original image, the liver region is created. In case of Tumor extraction, each pixel in the coarse segmentation output is binarized using dynamic thresholding, and a decision is made whether the pixel is tumor or normal.

3. RESULTS AND DISCUSSION

The proposed task is carried out using the MATLAB software with the system specification of 1.8 GHz processor and 2 GB of RAM. A real axial CT images are taken for experimental analysis and discussion. The proposed work runs for 60 datasets. The experimental results are discussed with different segmentation methods. The shape of the liver is complex, so some of the conventional methods fail to segment the liver contour. This conventional method needs more user interaction to segment the region of interest. The proposed methods overcome the drawbacks of the existing methods by combining one or more segmentation algorithms. The Neutrosophic set based FCM thresholding, utilizes a 3 class of FCM thresholding to obtain the binary image of the liver contour. Figure 5 illustrates the various processing steps in NS based FCM method. Figure 5(a) explains the preprocessed image and Figures 5(b) to (d) shows the different steps in NS based algorithm. Liver mask is shown in Figure 5(e) and superimposed image in Figure 5(f).

Totally three binary images are obtained after FCM thresholding of true, false, and indeterminate images. All these images are combined to get final binarized image. The largest region is identified, and liver mask is obtained. Using this mask, area of the pixels within the region has been calculated. This area calculation is compared with ground truth obtained from the experts. After finding the area of liver contour, volume measurement of liver has been calculated. The outline of liver contour is delineating.

In optimization-based liver segmentation, optimal cluster center is calculated using grey wolf method. In this method, we are reinforcing the importance of optimization approach to extract the liver contour. Reason of choosing this optimization method because of simple principle, easily way of implementation process, a smaller number of parameters. Firstly, the true image from NS domain has been taken for experiment analysis. These clusters are used to get the optimum threshold. These thresholds are used to segment the liver contour. Followed by this, area of ROI and volume measurement has been calculated. For implementation, we used the following parameters: *number of iterations=15*, *fuzziness=2*, *cluster centers=3*, *number of search agents=20* for optimization-based liver segmentation.

Figure 6 shows the output of optimization-based liver segmentation with preprocessed image in Figure 6(a). The results of true image in Figure 6(b) and binarized images in Figure 6(c). ROI and final liver mask are depicted in Figures 6(d) and (e). Superimposed image is outlined in Figure 6(f). By looking at the segmented output of all the methods, optimization-based liver system gives fine results. But the eye of the

mind recommends that optimization results are commendable in contrast with all other methods. This inference is completely based on visualization. A few more sample images and results for both the methods are shown in Figure 7. Liver with tumor contour is highlighted in Figure 7(a). Tumor region is delineated in Figure 7(b) with depth of tumor are point up in Figure 7(c). To analysis and visualize the tumor region in detail, contour labeling is done using MATLAB software. In contour labeling, x axis and y axis represent column and row pixel values.

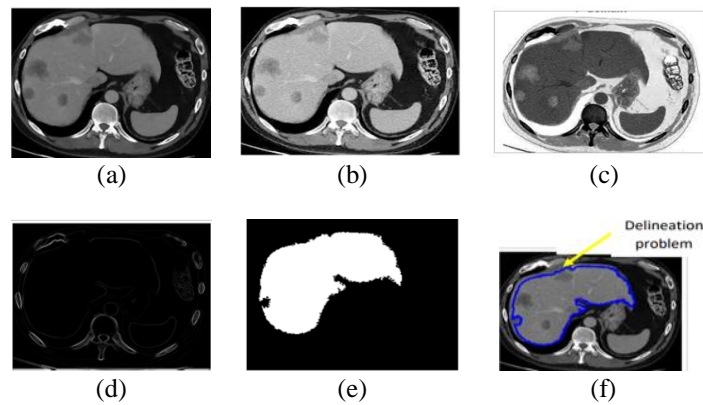


Figure 5. Results of NS based FCM thresholding method; (a) preprocessed image, (b) appropriate (true image), (c) false mage, (d) indeterminate image, (e) liver mask after LCC and post processing, and (f) superimposed image

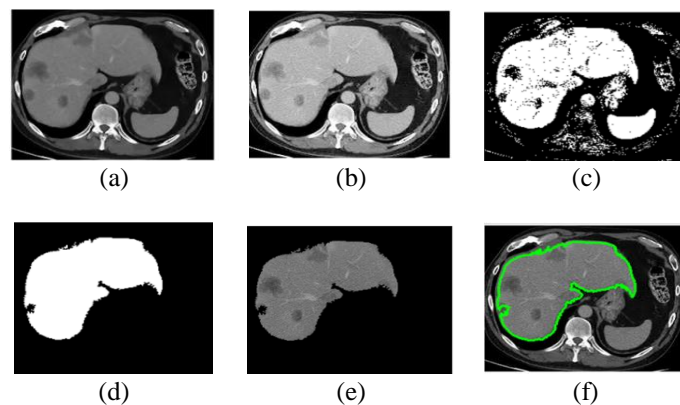


Figure 6. Results of optimization-based liver segmentation; (a) preprocessed image, (b) appropriate (true image), (c) binarized image after GWO and FCM, (d) ROI, (e) liver mask after LCC and post processing, and (f) superimposed image

To understand the best segmentation method, following performance measures [30], [31] are done and this analysis applicable for both normal and abnormal images. The dice coefficient is the most often used performance metric for evaluating the accuracy in segmented medical images. These metrics reveal the level upon which segmented picture "A" and expert-manually segmented image "M" overlap and resemble one another. Performance discussion might also include true positive rate and misclassification rate. These measurements are based purely on how often pixels appear in the common region. Sensitivity and recall are other names for true positive rate. And the reverse of true positive rate is misclassification rate.

Table 2 explains the performance of optimization-based grey wolf optimization-based liver segmentation (GWOLS) with NS based FCM. The average accuracy of both the methods are same in terms of dice coefficient and the true positive rate. From the table it can be inferred that the lower the misclassification rate, better is the segmentation results. The quantitative results of both the methods are relatively similar. But the NS based method lightly squeezed the contour sketch of region of interest and obtained the accuracy of 90.9% whereas optimization based GWOLS achieved the accuracy of 92.23% and comparative analysis are

shown in Figure 8. Figure 8(a) represent the performance measure in terms of dice coefficient with true positive rate in Figure 8(b). The performance of proposed method is verified with different liver image dataset taken from [32]. Both real and simulated liver dataset are taken for validation.

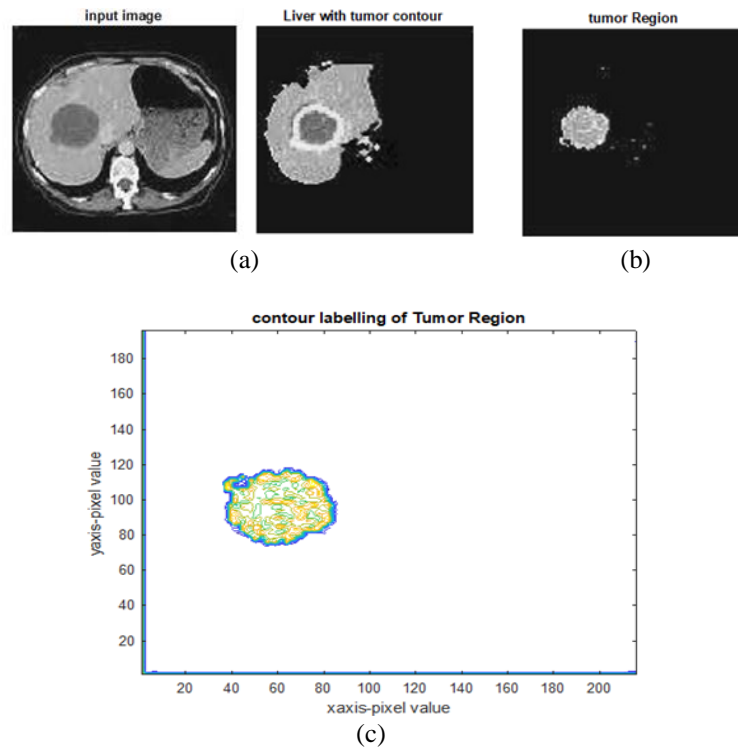


Figure 7. Visualization of tumor region: (a) liver contour with tumor, (b) extracted tumor region, and (c) contour labeling of tumor region

Table 2. Performance of NS based FCM and optimization based GWOLS

Database	NS Based FCM Method			Optimization based GWOLS		
	Dice	TPR	MCR	Dice	TPR	MCR
DB1	0.923	0.901	0.099	0.941	0.917	0.083
DB2	0.902	0.897	0.103	0.903	0.92	0.08
DB3	0.916	0.895	0.105	0.913	0.9927	0.073
DB4	0.898	0.907	0.093	0.922	0.928	0.072
DB5	0.896	0.899	0.101	0.934	0.932	0.065
Avg	0.909	0.899	0.102	0.9226	0.924	0.075

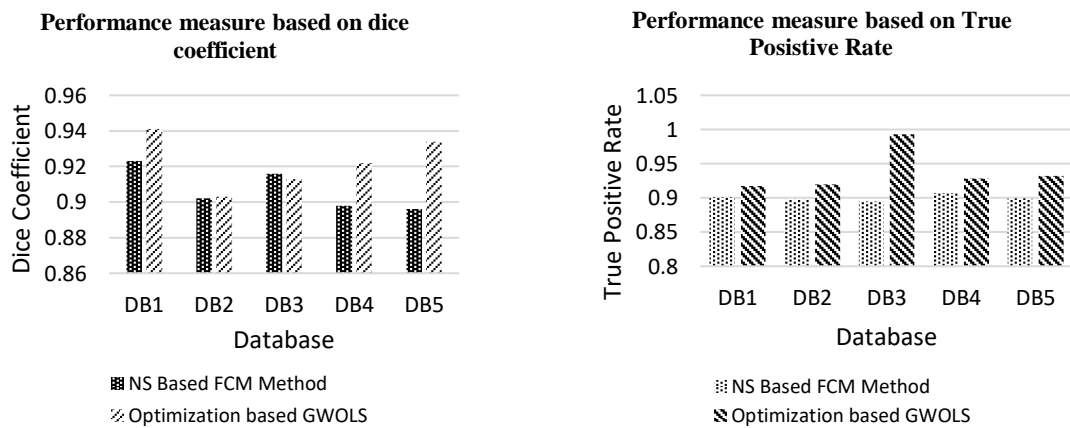


Figure 8. Comparative analysis using (a) dice coefficient and (b) true positive rate

Table 3 shows the computation time of both the algorithms. The performance of GWOLS was compared with NS based FCM and the results revealed that both the methods achieved the same accuracy but the computational time of GWOLS was more when compared to NS based FCM. But GWOLS method provides optimum results and takes less user interaction to segment the liver contour as well as tumor.

Table 3. Computation time of NS based FCM and optimization based GWOLS

Database	NS Based FCM Method		Optimization based GWOLS	
	Dice	Time (Sec)	Dice	Time (Sec)
DB1	0.923	33.87	0.941	54.28
DB2	0.902	32.11	0.903	60.45
DB3	0.916	33.26	0.913	71.23
DB4	0.898	32.96	0.922	62.89
DB5	0.896	33.12	0.934	61.34
Avg	0.909	33.064	0.9226	62.038

Table 4 provides the segmentation mode and the interaction level of each algorithm. It can be observed that dice coefficient of the proposed method is superior to that of other works. The mode explains segmentation process whether the technique is manual or semi or fully automatic. Interaction level helps to find the computation time spend by the user. This decides how much time user interaction is required. So, the proposed method comes under fully automatic technique with low interaction level. This method can delineate liver boundaries and found to be efficient than other state of the art methods.

Table 4. Segmentation mode and the interaction level of different techniques

Techniques	Mode	Interaction level	Dice Coefficient (%)
Level set	Semi	High	70
Region growing	Semi	Medium	84
FCM	Auto	Medium	87
K-means +LS	Auto	Low	88.32
Proposed Method	Auto	Low	92.23

4. CONCLUSION

This paper presented optimization-based segmentation method to traced the liver boundaries automatically. Whereas user based manual tracing takes more time nearly 30 to 45 minutes on average to trace the liver contour for calculating the liver volume. Sometime manual tracing gives subjective results and accuracy depends on radiologist's whether experienced or non-experienced. So, there is a demand of computer assisted system for extraction of liver contour to visualize the suspicious abnormal area inside the contour region. The proposed work helps to detect the liver as well as tumor region. In future, the proposed work can also be applied for other types of medical images and also optimization algorithm can be used in preprocessing and classification phase to get the accurate results.

REFERENCES

- [1] C. Barry, "Fatty liver disease: a growing health problem in India - causes, symptoms, diagnosis, treatment," *Medindia*, 2014. <https://www.medindia.net/patients/patientinfo/latest-publication-and-research-on-fatty-liver-disease.htm> (accessed Aug. 08, 2022).
- [2] WHO, "Hepatitis," World Health organization. https://www.who.int/health-topics/hepatitis#tab=tab_1 (accessed Aug. 08, 2022).
- [3] S. M. Atabo and A. A. Umar, "A review of imaging techniques in scientific research/clinical diagnosis," *MOJ Anatomy & Physiology*, vol. 6, no. 5, Oct. 2019, doi: 10.15406/mojap.2019.06.00269.
- [4] A. H. Foruzan, Y.-W. Chen, R. A. Zoroofi, and M. Kaibori, "Analysis of CT Images of Liver for surgical planning," *American Journal of Biomedical Engineering*, vol. 2, no. 2, pp. 23–28, Aug. 2012, doi: 10.5923/j.ajbe.20120202.05.
- [5] O. Diaz *et al.*, "Data preparation for artificial intelligence in medical imaging: A comprehensive guide to open-access platforms and tools," *Physica Medica*, vol. 83, pp. 25–37, Mar. 2021, doi: 10.1016/j.ejmp.2021.02.007.
- [6] K. R. Krishnan and S. Radhakrishnan, "Hybrid approach to classification of focal and diffused liver disorders using ultrasound images with wavelets and texture features," *IET Image Processing*, vol. 11, no. 7, pp. 530–538, Jul. 2017, doi: 10.1049/iet-ipr.2016.1072.
- [7] N. Elmenabawy, M. El-Seddek, H. E.-D. Moustafa, and A. Elnakib, "Deep segmentation of the liver and the hepatic tumors from abdomen tomography images," *International Journal of Electrical and Computer Engineering (IJECE)*, vol. 12, no. 1, pp. 303–310, Feb. 2022, doi: 10.11591/ijece.v12i1.pp303-310.
- [8] W. Wu, Z. Zhou, S. Wu, and Y. Zhang, "Automatic Liver segmentation on volumetric CT images using supervoxel-based graph cuts," *Computational and Mathematical Methods in Medicine*, vol. 2016, pp. 1–14, 2016, doi: 10.1155/2016/9093721.

- [9] A. F. Ali, A. Mostafa, G. I. Sayed, M. A. Elfattah, and A. E. Hassanien, "Nature inspired optimization algorithms for CT liver segmentation," in *Medical Imaging in Clinical Applications*, 2016, pp. 431–460, doi: 10.1007/978-3-319-33793-7_19.
- [10] G. I. Sayed, A. E. Hassanien, and G. Schaefer, "An automated computer-aided diagnosis system for abdominal CT liver images," *Procedia Computer Science*, vol. 90, pp. 68–73, 2016, doi: 10.1016/j.procs.2016.07.012.
- [11] S. Mirjalili, S. M. Mirjalili, and A. Lewis, "Grey wolf optimizer," *Advances in Engineering Software*, vol. 69, pp. 46–61, Mar. 2014, doi: 10.1016/j.advengsoft.2013.12.007.
- [12] S. S. Kumar, R. S. Moni, and J. Rajeesh, "Automatic liver and lesion segmentation: a primary step in diagnosis of liver diseases," *Signal, Image and Video Processing*, vol. 7, no. 1, pp. 163–172, Jan. 2013, doi: 10.1007/s11760-011-0223-y.
- [13] V. T.-T. Vo, H.-J. Yang, G.-S. Lee, S.-R. Kang, and S.-H. Kim, "Effects of multiple filters on liver tumor segmentation from CT images," *Frontiers in Oncology*, vol. 11, Oct. 2021, doi: 10.3389/fonc.2021.697178.
- [14] H. J. Abd, A. S. Abdullah, and M. S. S. Alkafaji, "A new swarm intelligence information technique for improving information balancedness on the skin lesions segmentation," *International Journal of Electrical and Computer Engineering (IJECE)*, vol. 10, no. 6, pp. 5703–5708, Dec. 2020, doi: 10.11591/ijece.v10i6.pp5703-5708.
- [15] M. Vera *et al.*, "Smart operator for the human liver automatic segmentation, present in medical images," *Journal of Physics: Conference Series*, vol. 1386, no. 1, Nov. 2019, doi: 10.1088/1742-6596/1386/1/012132.
- [16] J. Muthuswamy, "Extraction and classification of liver abnormality based on neutrosophic and SVM classifier," in *Progress in Advanced Computing and Intelligent Engineering*, 2019, pp. 269–279, doi: 10.1007/978-981-13-1708-8_25.
- [17] Boehringer Ingelheim Pharmaceuticals, "Radiology rounds," Boehringer Ingelheim Pharmaceuticals, 2016. <https://www.ipfradiologyrounds.com/hrct-primer/image-reconstruction/> (accessed Aug. 08, 2022).
- [18] Radiology cafe, "Anatomy of abdominal CT image." Radiology café, 2021. Accessed: Aug. 08, 2022. [Online]. Available: <https://www.radiologycafe.com/radiology-basics/imaging-modalities/ct-overview/>
- [19] A. Gielczyk, A. Marciniak, M. Tarczewska, and Z. Lutowski, "Pre-processing methods in chest X-ray image classification," *PLOS ONE*, vol. 17, no. 4, Apr. 2022, doi: 10.1371/journal.pone.0265949.
- [20] A. A. Adegun, S. Viriri, and R. O. Ogundokun, "Deep learning approach for medical image analysis," *Computational Intelligence and Neuroscience*, vol. 2021, pp. 1–9, May 2021, doi: 10.1155/2021/6215281.
- [21] C. Ning, S. Liu, and M. Qu, "Research on removing noise in medical image based on median filter method," in *2009 IEEE International Symposium on IT in Medicine & Education*, Aug. 2009, pp. 384–388, doi: 10.1109/ITIME.2009.5236393.
- [22] Y. Al-Saeed, H. Soliman, and M. Elmogy, "Liver segmentation using fast-generalized fuzzy C-means (FG-FCM) from CT scans," in *2020 International Conference on Data Analytics for Business and Industry: Way Towards a Sustainable Economy (ICDABI)*, Oct. 2020, pp. 1–6, doi: 10.1109/ICDABI51230.2020.9325703.
- [23] W. Alomoush, A. Alrosan, A. Almomani, K. Alissa, O. A. Khashan, and A. Al-Nawasrah, "Spatial information of fuzzy clustering based mean best artificial bee colony algorithm for phantom brain image segmentation," *International Journal of Electrical and Computer Engineering (IJECE)*, vol. 11, no. 5, pp. 4050–4058, Oct. 2021, doi: 10.11591/ijece.v11i5.pp4050-4058.
- [24] A. M. Anter and A. E. Hassenian, "CT liver tumor segmentation hybrid approach using neutrosophic sets, fast fuzzy c-means and adaptive watershed algorithm," *Artificial Intelligence in Medicine*, vol. 97, pp. 105–117, Jun. 2019, doi: 10.1016/j.artmed.2018.11.007.
- [25] G. I. Sayed and A. E. Hassanien, "Moth-flame swarm optimization with neutrosophic sets for automatic mitosis detection in breast cancer histology images," *Applied Intelligence*, vol. 47, no. 2, pp. 397–408, Sep. 2017, doi: 10.1007/s10489-017-0897-0.
- [26] T. Eelbode *et al.*, "Optimization for medical image segmentation: Theory and practice when evaluating with dice score or Jaccard index," *IEEE Transactions on Medical Imaging*, vol. 39, no. 11, pp. 3679–3690, Nov. 2020, doi: 10.1109/TMI.2020.3002417.
- [27] I. Ismail and A. H. Halim, "Comparative study of meta-heuristics optimization algorithm using benchmark function," *International Journal of Electrical and Computer Engineering (IJECE)*, vol. 7, no. 3, pp. 1643–1650, Jun. 2017, doi: 10.11591/ijece.v7i3.pp1643-1650.
- [28] M. Rela, S. Nagaraja Rao, and P. R. Reddy, "Optimized segmentation and classification for liver tumor segmentation and classification using opposition-based spotted hyena optimization," *International Journal of Imaging Systems and Technology*, vol. 31, no. 2, pp. 627–656, Jun. 2021, doi: 10.1002/ima.22519.
- [29] S. K. Siri and M. V. Latte, "A novel approach to extract exact liver image boundary from abdominal CT scan using neutrosophic set and fast marching method," *Journal of Intelligent Systems*, vol. 28, no. 4, pp. 517–532, Sep. 2019, doi: 10.1515/jisys-2017-0144.
- [30] A. A. Taha and A. Hanbury, "Metrics for evaluating 3D medical image segmentation: analysis, selection, and tool," *BMC Medical Imaging*, vol. 15, no. 1, Dec. 2015, doi: 10.1186/s12880-015-0068-x.
- [31] A. Gaber, H. A. Youness, A. Hamdy, H. M. Abdelaal, and A. M. Hassan, "Automatic classification of fatty liver disease based on supervised learning and genetic algorithm," *Applied Sciences*, vol. 12, no. 1, Jan. 2022, doi: 10.3390/app12010521.
- [32] Larxel, "Liver Tumor segmentation. 130 CT scans for liver tumor segmentation," Kaggle, 2021. <https://www.kaggle.com/datasets/andrewmvd/liver-tumor-segmentation> (accessed Dec. 10, 2022).

BIOGRAPHIES OF AUTHORS



Jayanthi Muthuswamy     received her Ph.D. degree in Electrical and Electronics Engineering, VTU University, Belagavi, India, 2019. She is currently working as Associate Professor in Electronics and communication Engineering, New Horizon College of Engineering, Bangalore. She has authored or coauthored more than 25 refereed journal and conference papers. Her research interests include digital signal processing, biomedical signal and image processing, IoT, and machine learning. She can be contacted at email: jayanthisathish1012@gmail.com.



Chanda Verabadra Reddy    received her Ph.D. degree in Electrical and Electronics Engineering VTU University, Belagavi, India, 2019. She has been a professor in Electronics and communication Engineering, K. S. Institute of Technology, under VTU University, since 2001. She is currently the IQAC coordinator. She has authored or coauthored more than 30 refereed journal and conference papers. Her research interests include fuzzy logic, artificial intelligence, and wireless communication. She can be contacted at chandavreddy@ksit.edu.in.



Rekha Narayanaswamy    received her Ph.D. degree in Electrical and Electronics Engineering VTU University, Belagavi, India, 2020. She is currently working as Associate Professor in Electronics and communication Engineering, K. S. Institute of Technology, under VTU University. She has authored or coauthored more than 20 refereed journal and conference papers. Her research interests include wireless and data communication, secure communication networks, MATLAB modeling and simulation. She can be contacted at rekhan@ksit.edu.in.